ADVANCES IN ATMOSPHERIC SCIENCES, VOL. 30, NO. 2, 2013, 280–290

Variability and Risk Analysis of Hong Kong Air Quality Based on Monsoon and El Niño Conditions

Jong-Suk KIM[1,2], ZHOU Wen*[1,2] (周 文), Ho Nam CHEUNG[1,2], and Chak Hang CHOW[1,2]

[1] *School of Energy and Environment, City University of Hong Kong, Hong Kong*

[2] *Guy Carpenter Asia-Pacific Climate Impact Centre, City University of Hong Kong, Hong Kong*

(Received 11 April 2012; revised 12 June 2012)

ABSTRACT

This study presents an exploratory analysis aimed at improving understanding of the variability of Hong Kong air quality associated with different climate conditions. Significantly negative correlations were found when Niño 3 led particulate matter $\leqslant$10 μm PM_{10}) and NO_2 by 2–3 months over the Hong Kong territory, while the other pollutants (e.g., O_3, SO_2) showed modest correlations. A significant decreasing trend in visibility was observed during the autumn and winter, which has potential implications for the air-quality degradation and the endangerment of human health in Hong Kong. In an El Niño summer, the visibility was relatively better, while visibility in other seasons was diminished. On the other hand, in La Niña events, significant changes occurred in visibility in winter and autumn. Air pollution indices were less sensitive to the South China Summer Monsoon (SCSM), but a relatively high correlation existed between the East Asian Winter Monsoon (EAWM) and air pollutants. Rainfall was lower during most of the strong EAWM years compared to the weak years. This result suggests that the pollutants that accumulate in Hong Kong are not easy to wash out, so concentrations remain at a higher level. Finally, based on the conditional Air Pollution Index (API) risk assessment, site-specific vulnerabilities were analyzed to facilitate the development of the air-quality warning systems in Hong Kong.

Key words: air quality, El Niño/La Niña, Monsoon, API risk, Hong Kong

Citation: Kim, J.-S., W. Zhou, H. N. Cheung, and C. H. Chow, 2013: Variability and risk analysis of Hong Kong air quality based on monsoon and El Niño conditions. *Adv. Atmos. Sci.*, **30**(2), 280–290, doi: 10.1007/s00376-012-2074-z.

1. Introduction

The weather and climate of Hong Kong are strongly dominated by the East Asian monsoons, which change the air mass flow and wind direction during winter and summer as a result of changes in the thermal structure over the Asian continent (Chan et al., 1998; Lam et al., 2001; Liu and Chan, 2002; Zhou et al., 2006, 2007; Gu et al., 2009a, b; Wang et al., 2009, 2010; Zhou et al., 2010; Wei et al., 2011; Yan et al., 2011; Zhu et al., 2011). With the rapid industrial and economic development in China, air pollution has emerged as a major environmental issue. In 2004, the results of air-quality research involving 360 cities showed that >75% of the urban population was exposed to air considered unsuitable for inhabited areas (Shao et al., 2006). The Pearl River Delta (PRD), located on the coast of South China, is one of the most highly urbanized and densely populated regions in China. In recent decades, this region has suffered increasingly serious air pollution problems (Chan and Yao, 2008; Deng et al., 2008), such as high aerosol concentrations and low visibility (Wu et al., 2006), which have received more and more attention from the public because of their adverse effects on health and environment.

The purposes of this study were (1) to classify the dominant climate patterns in South China and to characterize the links between the climate patterns and Hong Kong air quality, (2) to assess the differential impacts of South China summer and winter climate and weather conditions and El Niño or La Niña on Hong Kong air quality, and (3) to analyze the air-quality risk associated with South China Summer Monsoon

*Corresponding author: ZHOU Wen, wenzhou@cityu.edu.hk

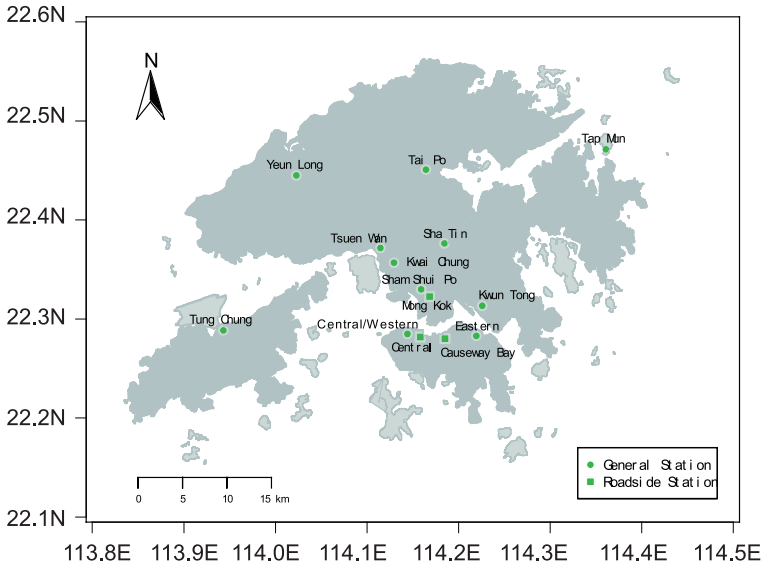

Fig. 1. Map of Hong Kong showing the ambient air-monitoring stations.

(SCSM) and East Asian Winter Monsoon (EAWM) circulations to provide tailored information that will contribute to the development of the air-quality warning system in Hong Kong.

2. Data and methodology

The analysis presented here was achieved by collecting air pollutant concentrations and meteorological data from representative monitoring sites (Fig. 1) that describe key climate elements and air pollutants in Hong Kong. Table 1 shows the monitoring station information. We used multivariate statistical techniques to identify the dominant patterns to determine the climate regimes that are closely related to high or low air-pollutant concentrations, and to estimate the relationship between the air quality in Hong Kong and the monsoon variability over South China, taking into consideration the role of the El Niño Southern Oscillation (ENSO) (Zhou and Chan, 2005; Zhou et al., 2006). The ENSO index, calculated from a 3-month running mean of the HadISST1 dataset (Rayner et al., 2003) in the Niño3 region (5°N–5°S, 90°–150°W), was used in this study. An El Niño event is defined by the Niño3 index exceeding the upper quartile (0.44) and persisting for six months from September to February. A La Niña event is identified by the same definition, but using the lower quartile (−0.63) as a threshold. According to this definition, we found eight El Niño events (1969/70, 1972/73, 1976/77, 1982/83, 1987/88, 1991/92, 1997/98, 2002/03) and five La Niña events (1970/71, 1973 / 74, 1975 / 76, 1988 / 89, 1999 / 2000).

Table 1. Station information.

No	Station Name	Latitude (°N)	Longitude (°E)	Remark
1	Central/Western	22.28	114.14	
2	Eastern	22.28	114.22	
3	Kwai Chung	22.36	114.13	
4	Kwun Tong	22.31	114.23	
5	Sha Tin	22.38	114.18	
6	Sham Shui Po	22.33	114.16	
7	Tai Po	22.45	114.16	
8	Tap Mun	22.47	114.36	
9	Tsuen Wan	22.37	114.11	
10	Tung Chung	22.29	113.94	
11	Yuen Long	22.44	114.02	
12	Causeway Bay	22.28	114.19	Roadside
13	Central	22.28	114.16	Roadside
14	Mong Kok	22.32	114.17	Roadside

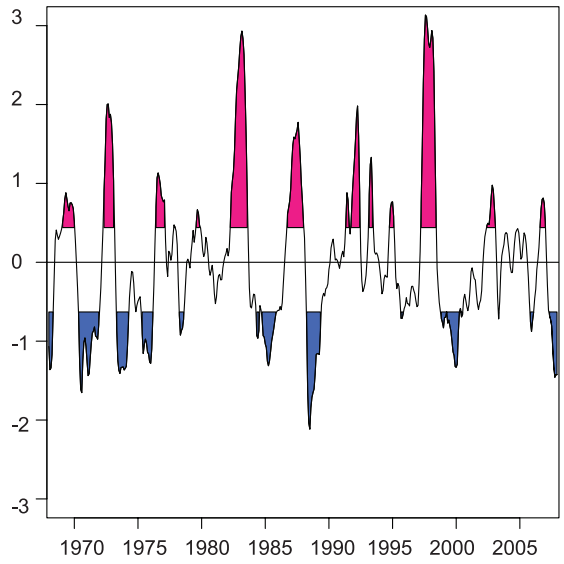

Fig. 2. Normalized time series of the Niño3 index during the period from 1968 to 2007. The solid line represents a 3-month moving average of the Niño3 index. The red shading indicates a Niño3 index greater than the upper quartile value (0.44), and blue shading shows a Niño3 index lower than the lower quartile value (−0.63).

Figure 2 shows the normalized time series of the Niño 3 index from 1968 to 2007. The levels of four pollutants were obtained from the Environmental Protection Department (EPD) to study the variations in different areas of Hong Kong during 2000–2009, i.e., particulate matter $\leqslant$10 μm (PM_{10}), O_3, NO_2, and SO_2. Quantile regression (QR; Koenker, 2005; Barbosa, 2008; Elsner et al., 2008; Kim and Jain, 2011) was used for trend analysis. The results from the QR provide detailed changes in the distribution, including tail probability changes and asymmetric trends for various quantiles of the response variables (Kim and Jain, 2010, 2011). Koenker (2005) also provided a detailed overview of this approach. A bootstrap method was used to test the statistical significance of the trend at the 90% confidence level. In this study, the visibility data obtained from Hong Kong Observatory were filtered to exclude observations affected by natural impairments such as early morning radiation fogs and high relative humidity (RH). Daylight visibility observations (1000–1400 LST) were filtered with RH <80% in a conservative manner (Dayan and Levy, 2005). In the following section, we explore the covariation between the ENSO and air pollution indices in Hong Kong.

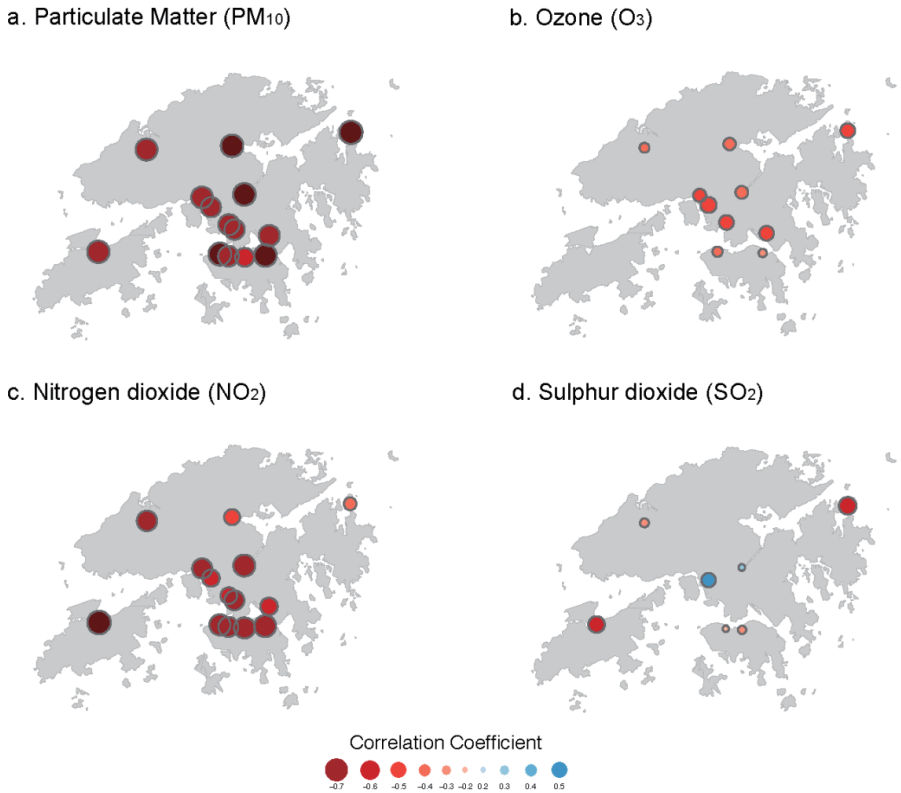

Fig. 3. Correlation between ENSO (lag −2) and air pollution indices (PM_{10}, O_3, NO_2, SO_2) in Hong Kong during the period 2001–2009. For each case, only values that are at least 90% significant are marked with a colored circle.

3. Impact of ENSO on air quality in Hong Kong

3.1 *Correlation analysis*

The cross-correlation, which provides a useful starting point for understanding the signal of large-scale climatic variability, was conducted to identify the relationship between ENSO and different pollutant concentrations in Hong Kong. The spatial pattern of correlation between the Niño3 and air pollution level is shown in Fig. 3. The maximum correlation coefficient was found when the Niño3 index led air pollutant concentrations by two months. The analysis indicated that there was a significant negative correlation between the Niño3 index and air pollutants, except for SO_2 at five stations (i.e., Kwai Chung, Kwung Tong, Sha Tin, Sham Shui Po, Tsuen Wan). A Pearson correlation analysis showed that PM_{10} and NO_2 had negative correlations with the Niño3 (ranging from −0.40 to −0.74) over the Hong Kong region, while the other pollutants showed modest correlations (refer to Table S1 in the supplementary information for more detail). Notably, the concentration of SO_2 has been decreasing over the past two decades due to the regulation of the sulfur content in transport and to the structural transition of the economy from manufacturing to services (Lau et al., 2005).

3.2 *Changes in visibility*

Because the EPD records do not go back far enough, visibility was used to represent the pollutant loadings. Atmospheric visibility has a significant correlation with pollutant concentrations (Dayan and Levy, 2005; Louie et al., 2005; Tsal, 2005; Lee et al., 2006; Leung and Lam, 2008; Leung et al., 2008; Fan et al., 2009; Wu et al., 2010). Table 2 shows the correlation results for the four air pollutants during 2001–2007. PM_{10} and NO_2 had negative correlations with visibility (ranging from −0.42 to −0.84), while O_3 and SO_2 showed modest correlations at some stations. Decreased visibility was significantly related with human health problems, such as cardiovascular disease, asthma, and compromised lung function (Samet and Krewski, 2007). Figure 4 presents trends in the seasonal visibility across key quantiles (i.e., median, upper and lower quartiles) from 1968 to 2007. There was a significant downward trend in visibility during autumn and winter, whereas an upward trend occurred in the median and upper quartiles of summertime visibility. However, the lower quartile-based trend analysis showed no significant trends in visibility during summer. No significant shift in the median visibility was seen during the spring season. On the other hand, springtime visibility showed a statistically significant increase in the upper quartile and a statistically significant decrease in the lower quartile. Other approaches, such as the Mann–Kendall (MK) test and simple linear regression detecting monotonic trend in a time series provided an incomplete summary of trends, especially in cases where changes in tail distribution were apparent, while other quantiles showed no significant change in the response variable. In every season except summer, the lower quartiles of visibility showed statistically significant decreasing trends with potential implications for air contamination and the endangerment of human health in Hong Kong.

Figure 5 shows the empirical probability distribution of visibility anomalies (shown as a percentage of normal) for each season, with respect to the

Table 2. Correlation between air pollution indices and visibility during 2001–2007.

No	Station Name	PM_{10}	O_3	NO_2	SO_2
1	Central/Western	**−0.81**	**−0.41**	**−0.84**	−0.03
2	Eastern	**−0.80**	**−0.35**	**−0.82**	0.01
3	Kwai Chung	**−0.74**	**−0.53**	**−0.61**	**0.35**
4	Kwun Tong	**−0.77**	**−0.58**	**−0.68**	**0.22**
5	Sha Tin	**−0.79**	**−0.44**	**−0.83**	0.13
6	Sham Shui Po	**−0.70**	**−0.64**	**−0.59**	**0.22**
7	Tai Po	**−0.72**	**−0.44**	**−0.48**	0.00
8	Tap Mun	**−0.74**	**−0.60**	**−0.42**	**−0.30**
9	Tsuen Wan	**−0.76**	**−0.43**	**−0.78**	0.04
10	Tung Chung	**−0.72**	−0.17	**−0.75**	**−0.52**
11	Yuen Long	**−0.71**	**−0.27**	**−0.72**	**−0.29**
12	Causeway Bay	**−0.67**	NA	**−0.74**	−0.20
13	Central	**−0.74**	NA	**−0.73**	−0.19
14	Mong Kok	**−0.76**	NA	**−0.75**	−0.09

* Correlation estimates shown in boldface is statistically significant at the 5% level.

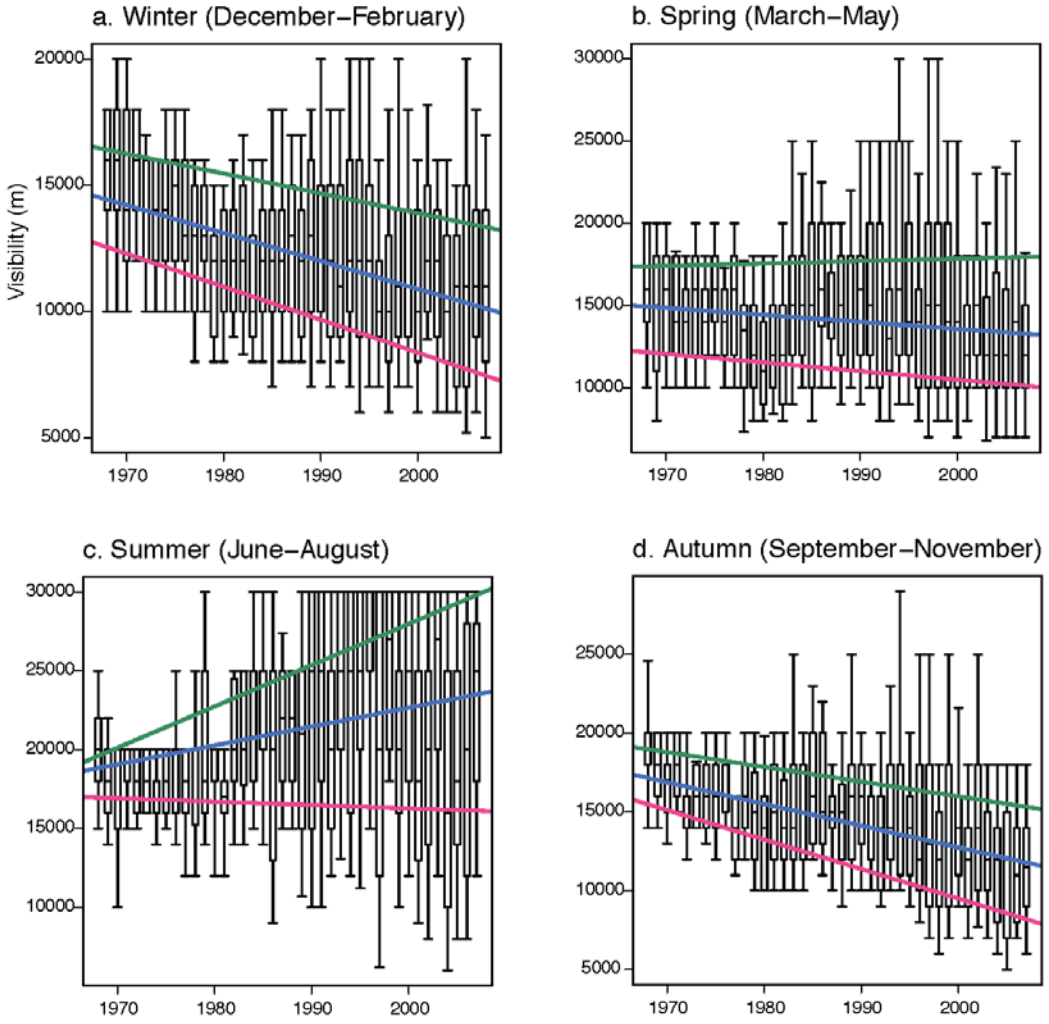

Fig. 4. Trend in seasonal visibility during 1968–2007. Trend lines are shown for lower quartile (in red), median (in blue), and upper quartile (in green). For each year, the variability is summarized using a boxplot (0.1, 0.25, 0.5, 0.75, 0.9 quartile levels are shown).

base period 1968–2007. The empirical probability density function (PDF) was estimated using Kernel density, one of the most widely used nonparametric techniques in theoretical and applied statistics (Bowman and Azzalini, 1997). The percentile change in visibility and the coefficient of variation (COV), which is a normalized measure of dispersion of the probability distribution, are also summarized in Table 3. For the El Niño years, negative anomalies in visibility, which may have implications for degraded air quality, were found in winter (December to February; DJF), spring (March to May; MAM), and autumn (September to November; SON), while summer (June to August; JJA) visibility showed a positive anomaly. In El Niño summer (composite mean: 1.02%), the visibility was slightly better than in La Niña years (composite mean: −3.86%), but the variability in summer visibility was also higher (COV: 25.36) than in La Niña years (COV: 2.75). Because tropical cyclones are likely to shift eastward, staying away from China during El Niño years (Elsner and Liu, 2003), the effect caused by the outermost suppression of tropical cyclones (TCs) and the change of wind field would be reduced, and would have a positive effect on improving the visibility in summer. However, the episodic TCs explain only modest changes in mean of summer visibility. The highest and lowest variations in visibility were found in winter and autumn, respectively, with a coefficient of variation (COV) of 19.21 (1.66) during El Niño years. In contrast, positive anomalies and low variations in visibility during winter (mean: 5.29%, COV: 1.59), spring (mean: 1.95, COV: 1.58), and autumn (mean: 5.18, COV: 1.27) were seen for La Niña years, which led to the opposite situation (neg-

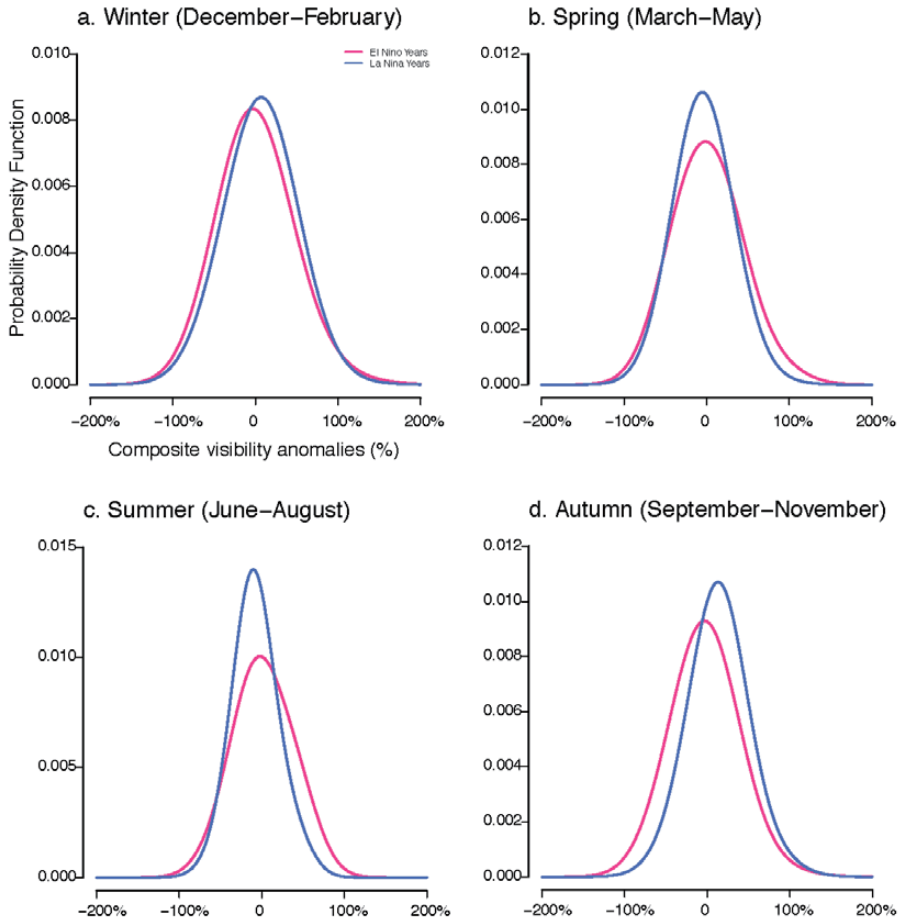

Fig. 5. Empirical probability density function for the seasonal composite visibility anomalies. The red line represents the distribution of visibility anomalies during El Niño years. The solid line in blue shows visibility anomalies in the phase of the La Niña.

ative anomalies and high variations in visibility) to that in El Niño years. During La Niña years, positive visibility in winter and autumn indicated statistically significant results at the 5% confidence level. Summer visibility (mean: −3.86%, COV: 2.75) was diminished in La Niña years, but this change was not found to be statistically significant. In autumn, the difference of the mean visibility between El Niño and La Niña years shows statistical significance at the 5% level.

In this study, one main concern regarding the consequences of climate change is the potential decrease in air quality. Although the impact of the ENSO on regional air quality is complicated, we expect that the conditional distribution of visibility presented here might provide useful information for the development of air-quality management systems in a changing cli-

Table 3. Summary statistics in seasonal visibility.

ENSO type	Statistics	Seasonal visibility			
		DJF	MAM	JJA	SON
El Niño years	Mean (%)	−0.43	−0.84	1.02	−3.70
	COV	19.21	10.77	15.36	1.66
La Niña years	Mean (%)	**5.29**	1.95	−3.86	**5.18**
	COV	1.59	1.58	2.75	1.27

* COV: the ratio of standard deviation to mean

Composite mean shown in boldface is statistically significant at the 5% level.

mate. In the next section, we discuss the relationship between the monsoon and air quality in Hong Kong.

4. Impact of monsoon on air quality in Hong Kong

4.1 *Rank analysis*

To assess the relationship between the monsoon and air-pollution episodes, we applied the rank-based approach. The observations from three stations were used to investigate the air quality in Hong Kong from general (Sha Tin), rural (Tap Mun), and roadside (Mong Kok) areas. In Fig. 6, the data from the Sha Tin station are arranged according to the monsoon index (Lu and Chan, 1999) during the June–August season. The four air-pollution indices in the June to August timeframe are shown below that, followed by the three meteorological indices. This arrangement demonstrates the sensitivity of air pollutants to seasonal climatic variations. For positive anomalies in the SCSM (departure from a long-term average for 2001–2009), all four pollutants were recorded as above average: all four pollutants were recorded as above average: 6 of the 14 events (42.9%) had above normal PM_{10} [mean (μ): 1.10 μg m^{-3}, standard deviation (σ): 6.86 μg m^{-3}]; and 8 of the 15 events had positive anomalies in O_3 (μ: 0.29, σ: 4.40). Positive anomalies were also observed in NO_2 (μ: 1.39, σ: 7.58) and SO_2 (μ: 0.68, σ: 8.68). Summer rainfall also showed a positive anomaly, with a mean value of 26.77 mm per month, but its variation was relatively high (σ: 287.76 mm month^{-1}). The variability in the four air pollutants was highest for O_3, which had a coefficient of variation (COV; the ratio of σ to μ) of 15.17, while the COV of the other pollutants ranged from 5.45 to 12.76 (PM_{10}: 6.24, NO_2: 5.45, SO_2: 12.76). In contrast, for negative SCSM anomalies, the air pollutants were more likely to show levels less than the long-term normal (PM_{10}: -1.19, O_3: -0.32, NO_2: -1.50, SO_2: -0.73), and their variations were lower than for positive SCSM anomalies, except for O_3. For the Tap Mun and Mong Kok stations, the impact of the four pollutant levels had an appreciable amount of scatter (Figs. S1 and S2 in Supplementary Information), so the relationships between the air-pollutant parameters and the SCSM were less clear. There was a somewhat unclear tendency in the rainfall pattern during the strong and weak monsoon years. In summer, rainfall is contributed mainly by the monsoon trough associated with the active southwesterly monsoon. In addition, the contribution of the rainfall from the trop-

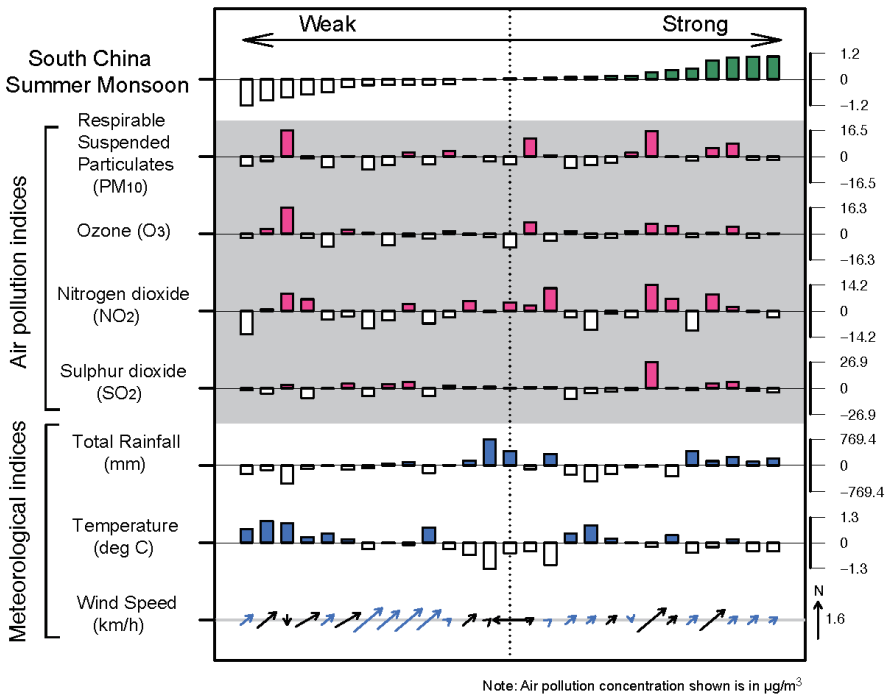

Fig. 6. Air pollution and weather indices for the Sha Tin monitoring station during 2001–2009. The data have been arranged by the South China Summer Monsoon (SCSM) index during the June–August season. The above-normal data are shaded with different colors (green, red, and blue).

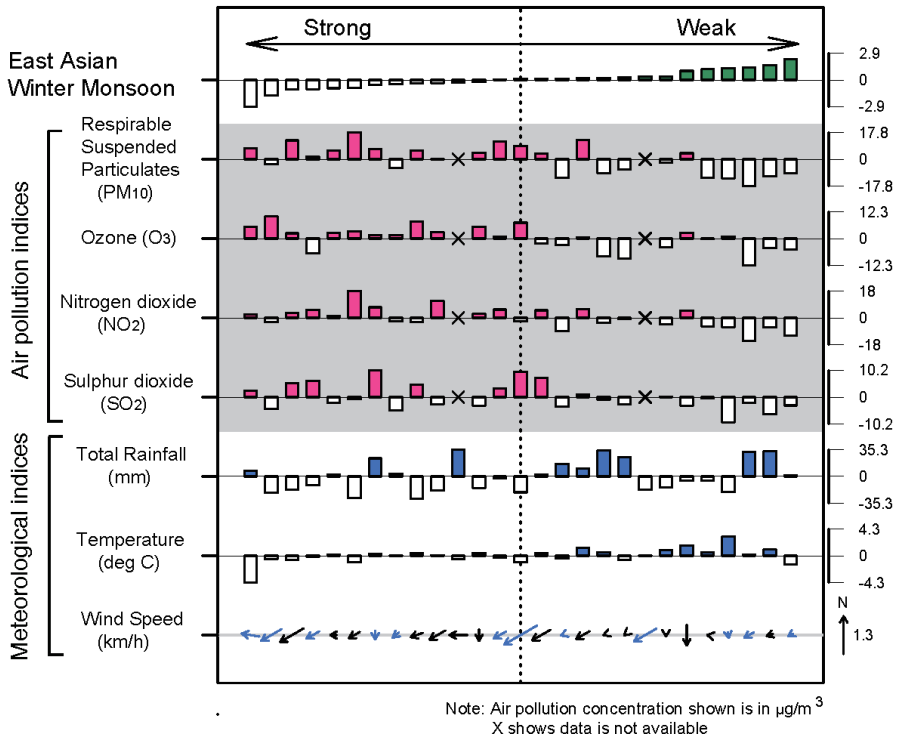

Fig. 7. Air pollution and weather indices for the Sha Tin monitoring station during 2000–2009. The data have been arranged by the East Asian Winter Monsoon (EAWM) index during the December–February season.

ical cyclones should not be neglected. Therefore, the strength of the SCSM cannot be considered the most outstanding factor affecting the general air quality in Hong Kong during summer.

Figure 7 shows the relationship between the EAWM and air pollution indices for the Sha Tin station. The monsoon index is defined as the area-averaged meridional wind over the South China (7.5°–20°N, 107.5°–120°E; Lu and Chan, 1999). As the strength of the EAWM is determined by the magnitude of the northerly wind, a stronger EAWM is characterized by a more negative value of the above index. The EAWM index is arranged in a similar way as in Fig. 6. The strong EAWM (in this case, negative anomalies) was accompanied by lower air-quality levels at Sha Tin: 8 of 10 events indicate above normal PM_{10} (μ: 4.79, σ: 6.72), and 9 of 10 events show positive anomalies in O_3 (μ: 3.28, σ: 4.29). There are also positive anomalies in NO_2 (μ: 3.98, σ: 6.37) and SO_2 (μ: 0.95, σ: 5.05). The variability of the four air pollutants was highest for SO_2, which had a COV of 5.32, while the COV of the other pollutants ranged from 1.31 to 1.60 (PM_{10}: 1.40, O_3: 1.31, NO_2: 1.60). In contrast, for positive EAWM monsoon anomalies, air-pollutant levels were likely to be less than the long-term normal (PM_{10}: −3.76, O_3: −2.58, NO_2: −3.12, SO_2: −0.75), while their variations are higher than for negative EAWM monsoon anomalies. The same tendency was also identified at Tap Mun and Mong Kok stations (refer to Figures S3 and S4 in Supplementary Information). During the strong winter monsoon seasons, high concentrations of polyaromatic hydrocarbons were mainly affected by local emissions from local sources superimposed on heavily polluted air masses from the mainland (Guo et al., 2003), because continental air masses could be carried to Hong Kong by a stronger northerly wind. Furthermore, most of the strong EAWM years in our study period suffered from less rainfall compared to the weak years. This suggests that the pollutants accumulated in Hong Kong were not easy to wash out, so that concentrations remained at a higher level.

4.2 *API risk analysis*

The Air Pollution Index (API) is defined by the highest index calculated by each of the five major pollutants (NO_2, SO_2, O_3, CO_2, and PM_{10}), with their respective health related air-quality objectives based on the Air Pollution Control Ordinance. The API is a simple way to describe air pollutant levels with a single number ranging from 0 to 500. An API number of 100 is particularly significant, because one or more

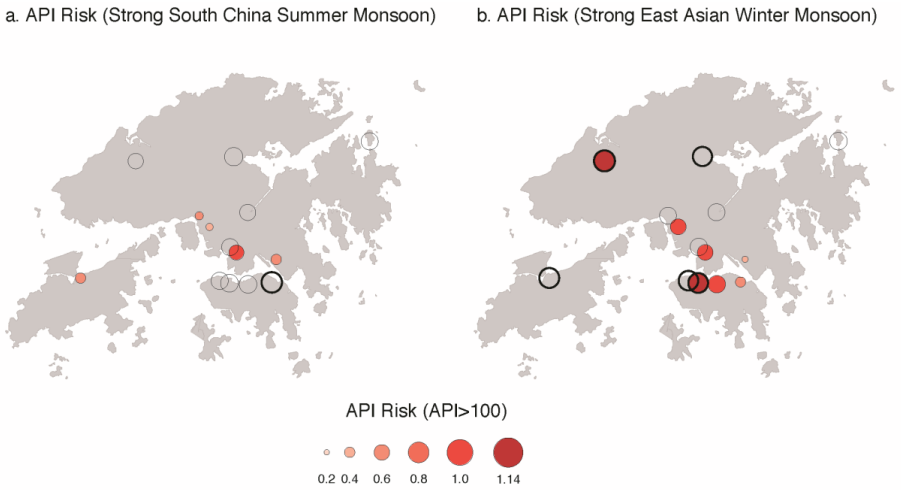

Fig. 8. API risk based on summer/winter monsoon. Red circles indicate statistical significance (p <0.10). Black circles represent API risk value >1.0. Unfilled circles indicate that there is not statistical evidence for API risk.

pollutants may pose immediate health effects to some susceptible residents in Hong Kong[a]. The potential health effects regarding the API are described in Table S2 in the Supplementary Section. In this study, we used a non-parametric Kernel approach that is widely used in theoretical and applied statistics (Bowman and Azzalini, 1997) to determine the risk of the API (Sen Gupta et al., 2011). The API risk was estimated by considering the ratio of the exceedance probability of the API based on the conditional distribution (API⩾100) to that of the unconditional API distribution.

$$\text{API Risk} = \frac{\text{P}[(\text{API} \geqslant \text{API}_{100}|\text{SM})]}{\text{P}(\text{API} \geqslant \text{API}_{100})} ,$$

where SM denotes strong monsoon, which is characterized by at least a half standard deviation stronger surface northerly and southerly wind over the northern part of the South China Sea than normal in winter and summer respectively (Lu and Chan, 1999).

Here, API is the air pollution index, ranging from 0 to 500. API_{100} is the air pollution level that may cause serious health problems to people with existing heart or respiratory illnesses. The strong monsoon was defined by rank analysis for the SCSM index (>0.66 quantile; 9 out of 27 events) and the EAWM index (<0.33 quantile; 9 of 27 events) for the period 2001–2009.

Figure 8 indicates that the conditional API risk associated with the strong summer and winter monsoons varies from station to station. For the strong SCSM, 13 of the 14 stations showed low API risk (<1.0), ranging from 0.39 to 0.99 (μ: 0.78, σ: 0.21). The eastern station showed a relatively high API risk (1.11), but it was not statistically significant. On the other hand, for the strong EAWM, 5 of the 14 stations showed a relatively high API risk, ranging from 1.04 to 1.14. The most significant change was seen in the Yuen Long station (API risk: 1.14), followed by the Central station (API risk: 1.07). The API risk analysis showed a relatively strong impact of the winter monsoon on API, but a less clear impact of the summer monsoon.

5. Summary and Conclusions

In this study, we found evidence to indicate that the air quality of Hong Kong appears to be significantly influenced by the South China Monsoon and ENSO. To recapitulate briefly, the results presented here may be summarized as follows:

(1) The results of the cross-correlation analysis indicated a negative sign in the correlation coefficient when the ENSO led air pollutant concentrations by two months (Fig. 3).

(2) For each season except summer, the lower quartile of visibility showed a positive trend with potential implications for the endangerment of human health in Hong Kong (Fig. 4). During the El Niño years, changes in visibility showed an opposite trend between summer and the other seasons. In El Niño summers, a relatively better visibility was apparent, while visibility in other seasons was diminished in the year of El Niño events. In contrast, for the La Niña years, significant changes in visibility were found in winter and autumn, a situation opposite (negative anomalies and high variations in visibility) to that in the El Niño years (Fig. 5

[a]API : Advice to public: http://www.epd-asg.gov.hk/english/advice/advice.html

and Table 3).

(4) The rank analysis showed that air pollution indices were less sensitive to the summer monsoon (Fig. 6), but a relatively good relationship existed between the winter monsoon and air pollutants (Fig. 7).

(5) Based on the conditional API risk assessment, specific vulnerabilities were diagnosed (Fig. 8). The API risk analysis showed a relatively strong impact of the EAWM on API, but a less clear impact of the SCSM.

The Earth system has been experiencing unprecedented changes that are important in modifying the global climate system and that have socioeconomic consequences for natural and human systems. Despite its limited sample size, we believe that the present study provides useful information, not only for Hong Kong but also for other regions for development of station-specific management systems for air quality in a changing climate. However, further studies based on robust numerical simulations are required to determine the synergistic impacts of the monsoon and ENSO on air quality.

Acknowledgements. This research was fully supported by HKSAR Department of Environment and Conservation Fund (ECF), Project 9211008: "Impacts of South China Monsoon Climate Variability and El Niño on Hong Kong Air Quality."

REFERENCES

Barbosa, S. M., 2008: Quantile trends in Baltic sea level. *Geophys. Res. Lett.*, **35**, L22704.

Bowman, A. W., and A. Azzalini, 1997: *Applied Smoothing Techniques for Data Analysis: The Kernel Approach with S-Plus illustrations.* Oxford University Press, Oxford, UK, 193pp.

Chan, C. K., and X. H. Yao, 2008: Air pollution in mega cities in China. *Atmos. Environ.*, **42**(1), 1–42.

Chan, L. Y., C. Y. Chan, and Y. Qin, 1998: Surface ozone pattern in Hong Kong. *J. Appl. Meteor.*, **37**, 1153–1165.

Dayan, U., and I. Levy, 2005: The influence of meteorological conditions and atmospheric circulation types on PM10 and visibility in Tel Aviv. *J. Appl. Meteor.*, **44**, 606–619.

Deng, X. J., and Coauthors, 2008: Effects of Southeast Asia biomass burning on aerosols and ozone concentrations over the Pearl River Delta (PRD) region. *Atmos. Environ.*, **42**(36), 8493–8501.

Elsner, J. B., J. P. Kossin, and T. H. Jagger, 2008: The increasing intensity of the strongest tropical cyclones. *Nature*, **455**, doi: 10.1038/nature07234.

Elsner, J. B., and K. B. Liu, 2003: Examining the ENSO-typhoon hypothesis. *Climate Research*, **25**, 43–54.

Fan, X. Q., Z. B. Sun, and M. F. Su, 2009: A new method to discern haze using meteorological parameters and air pollution factors, 2009 1st International Conference on Information Science and Engineering, 4640–4656.

Gu, W., C. Y. Li, W. J. Li, W. Zhou, and J. C. L. Chan, 2009a: Interdecadal unstationary relationship between NAO and east China's summer precipitation patterns. *Geophys. Res. Lett.*, **36**, L13702. doi: 10.1029/2009GL038843.

Gu, W., C. Y. Li, X. Wang, W. Zhou, and W. J. Li, 2009b: Linkage between Mei-yu precipitation and North Atlantic SST on the decadal timescale. *Adv. Atmos. Sci.,* **26**, 101–108, doi: 10.1007/s00376-009-0101-5.

Guo, H., S. C. Lee, K. F. Ho, X. M. Wang, and S. C. Zou, 2003: Particle-associated polycyclic aromatic hydrocarbons in urban air of Hong Kong. *Atmos. Environ.*, **37**(38), 5307–5317.

Kim, J. S., and S. Jain, 2010: High-resolution streamflow trend analysis applicable to annual decision calendars: a western United States case study. *Climatic Change*, **102**, 699–707.

Kim, J. S., and S. Jain, 2011: Precipitation trends over the Korean peninsula: Typhoon-induced changes and a typology for characterizing climate-related risk. *Environ. Res. Lett.*, **6**, 034033, doi: 10.1088/1748-9326/6/3/034033.

Koenker, R., 2005: *Quantile Regression*, Cambridge University Press, New York, 366pp.

Lam, K. S., T. J. Wang, L. Y. Chan, T. Wang, and J. Harris, 2001: Flow patterns influencing the seasonal behavior of surface ozone and carbon monoxide at a coastal site near Hong Kong. *Atmos. Environ.*, **35**, 3121–3135.

Lau, K. H, W. M. Wu, C. H. Fung, R. C. Henry, and B. Barron, 2005: Significant marine source for SO_2 levels in Hong Kong, Civic-exchange Environmental and Conservation reports. [Available online at http://www.civic-exchange.org/eng/upload/files/200506_MarineSourceSO2.pdf]

Lee, T. C., W. M. Leung, and K. W. Chan, 2006: Climatological normal for Hong Kong 1971–2000, Hong Kong Observatory Technical Note (Local), 83, 31pp.

Leung, Y. K., and C. Y. Lam, 2008: Visibility impairment in Hong Kong – A wind attribution analysis. *Bulletin of Hong Kong Meteorological Society*, **18**, 33–48.

Leung, Y. K., and M. C. Wu, and K. K. Yeung, 2008: A study on the relationship among visibility, atmospheric suspended particulate concentration and meteorological conditions in Hong Kong. *Acta Meteorologica Sinica*, **66**, 461–469. (in Chinese)

Liu, H., and J. C. L. Chan, 2002: An investigation of air-pollutant patterns under sea-land breezes during a severe air-pollution episode in Hong Kong. *Atmos. Environ.*, **36**(4), 591–601.

Louie, P. K. K., J. C. Chow, A. L. W. Chen, J. G. Watson, and D. W. M. Sin, 2005: PM 2.5 chemical composition in Hong Kong: Urban and regional variations. *Science of the Total Environment,* **338**, 267–281.

Lu, E., and J. C. L. Chan, 1999: A unified monsoon index for South China. *J. Climate*, **12**, 2375–2385.

Rayner, N. A., D. E. Parker, E. B. Horton, C. K. Folland, L.V. Alexander, D. P. Rowell, E. C. Kent, and A. Kaplan, 2003: Global analyses of sea surface temperature, sea ice, and night marine air temperature since the late nineteenth century. *J. Geophys. Res.*, **108**(D14), 4407, doi: 10.1029/2002JD002670.

Samet, J., and D. Krewski, 2007: Health effects associated with exposure to ambient air pollution. *Journal of Toxicology and Environment Health* (*Part A*), **70**, 227–242.

Sen Gupta, A., S. Jain, and J. S. Kim, 2011: Past climate, future perspective: An exploratory analysis using climate proxies and drought risk assessment to inform water resources management and policy in Maine, USA. *Journal of Environmental Management*, **92**, 941–947.

Shao, M., X. Y. Tang, Y. H. Zhang, and W. J. Lia, 2006: City clusters in China: Air and surface water pollution. *Frontiers in Ecology and the Environment*, **4**(7), 353–361.

Tsal, Y. I., 2005: Atmospheric visibility trends in a urban area in Taiwan 1961–2003. *Atmos. Environ.*, **39**(30), 5555–5567.

Wang, L., W. Chen, W. Zhou, and R. H. Huang, 2009: Interannual variations of East Asian though axis at 500-hPa and its association with the East Asian winter monsoon pathway. *J. Climate*, **22**, 600–614.

Wang, L., W. Chen, W. Zhou, J. C. L. Chan, D. Barriopedro, and R. H. Huang, 2010: Effect of the climate shift around mid 1970s on the relationship between wintertime Ural blocking circulation and East Asian climate. *Int. J. Climatol.*, **30**, 153–158.

Wei, K., W. Chen, and W. Zhou, 2011: Changes in the East Asian cold season since 2000. *Adv. Atmos. Sci.*, **28**, 69–79. doi: 10.1007/s00376-010-9232-y.

Wu, D., X. Y. Bi, and X. J. Deng, 2006: Effect of atmospheric haze on the deterioration of visibility over the Pearl River Delta. *Acta Meteorologica Sinica*, **64**(4), 510–516. (in Chinese)

Wu, Q. Z., Z. F. Wang, A. Gbaguidi, X. Tang, and W. Zhou, 2010: Numerical study of the effect of traffic restriction on air quality in Beijing. *SOLA*, **6A**, 17–20.

Yan, Z. W., J. J. Xia, C. Qian, and W. Zhou, 2011: Changes in seasonal cycle and extremes in China during the period 1960–2008. *Adv. Atmos. Sci.*, **28**, 269–283. doi: 10.1007/s00376-010-0006-3.

Zhou, L. T., F. Tam., W. Zhou, and J. C. L. Chan, 2010: Influence of South China Sea SST and the ENSO on winter rainfall over South China. *Adv. Atmos. Sci.*, **27**, 832–844. doi: 10.1007/s00376-009-9102-7.

Zhou, W., and J. C. L. Chan, 2005: Intraseaonal oscillations and the South China Sea summer monsoon onset. *Int. J. Climatol.*, **25**, 1585–1609.

Zhou, W., and J. C. L. Chan, 2007: ENSO and South China Sea summer monsoon onset. *Int. J. Climatol.*, **27,** 157–167.

Zhou, W., C. Y. Li, and J. C. L. Chan, 2006: The interdecadal variations of the summer monsoon rainfall over South China. *Meteor. Atmos. Phys.*, **93**, 165–175.

Zhou, W., C. Y. Li, and X. Wang, 2007: Possible connection between Pacific oceanic interdecadal pathway and East Asian winter monsoon. *Geophys. Res. Lett.*, **34**, L01701. doi: 10.1029/2006GL027809.

Zhu, Y. L., H. J. Wang, W. Zhou, and J. H. Ma, 2011: Recent changes in the summer precipitation pattern in east China and the background circulation. *Climate Dyn.*, **36**, 1463–1473.